

Alterations of the extracellular matrix of lung during zinc deficiency

Verónica S. Biaggio¹, Natalia R. Salvetti², María V. Pérez Chaca¹, Susana R. Valdez³, Hugo H. Ortega², María S. Gimenez^{1*} and Nidia N. Gomez^{1*}

¹*Departamento de y Bioquímica Ciencias Biológicas, Facultad de Química, Bioquímica y Farmacia, Universidad Nacional de San Luis, IMIBIO-CONICET, San Luis, Argentina*

²*Facultad de Ciencias Veterinarias, Universidad Nacional del Litoral, CONICET-Esperanza, Santa Fe, Argentina*

³*Instituto de Ciencias Básicas, Universidad Nacional de Cuyo, Centro Científico Tecnológico (CCT), CONICET-Mendoza, Argentina*

(Submitted 18 October 2010 – Final revision received 23 August 2011 – Accepted 23 August 2011 – First published online 12 October 2011)

Abstract

Suboptimal intake of Zn is one of the most common nutritional problems worldwide. Previously, we have shown that Zn deficiency (ZD) produces oxidative and nitrosative stress in the lung of rats. We analyse the effect of moderate ZD on the expression of several intermediate filaments of the cytoskeleton, as well as the effect of restoring Zn during the refeeding period. Adult male rats were divided into three groups: Zn-adequate control (CO) group; ZD group; Zn-refeeding group. CerbB-2 and proliferating cell nuclear antigen (PCNA) expression was increased in the ZD group while the other parameters did not change. During the refeeding time, CerbB-2, cytokeratins, vimentin and PCNA immunostaining was higher than that in the CO group. The present findings indicate that the overexpression of some markers could lead to the fibrotic process in the lung. Perhaps ZD implications must be taken into account in health interventions because an inflammation environment is associated with ZD in the lung.

Key words: CerbB-2: Pan-cadherins: Cytokeratins: Intermediate filaments: Proliferating cell nuclear antigen: Zinc deficiency: Lungs

Zn is an essential micronutrient, which may exert an anti-oxidant activity as demonstrated in defined chemical and cell culture systems, as well as *in vivo*⁽¹⁾. Therefore, the maintenance of discrete subcellular pools of Zn is critical for the functional and structural integrity of cells and contributes to a number of important biological processes⁽²⁾. Due to its anti-oxidant, anti-apoptotic and membrane-stabilising activities, it has been hypothesised that Zn protects the endothelium against oxidative stress by maintaining the integrity of endothelial cells⁽³⁾.

On the other hand, lung epithelial cells (pneumocytes) are responsible for the gas exchange in lungs. Chronic injury induces damage and subsequent loss of parenchymal cells⁽⁴⁾. Damage to lung epithelium is associated with interstitial oedema, leucocyte invasion and decreased gas exchange. This situation has been demonstrated in Zn-deficient (ZD) rats, with a significant oxidative and nitrosative stress⁽⁵⁾. In addition, these recruited inflammatory cells increase local concentration of transforming growth factor (TGF)- β 1, which causes the re-organisation and activation of pulmonary fibroblasts. Besides, the increase in reactive oxygen species production is

associated with the direct activation of pro-fibrogenic genes that produce collagen and with the decrease in endogenous antioxidants that have a protective role⁽⁴⁾. Previously, we analysed the expression of antioxidant enzymes in ZD lung⁽⁶⁾.

Resolution of alveolar epithelial/capillary membrane damage after lung injury requires coordinated and effective tissue reconstruction to re-establish a functional barrier. Several lines of investigation suggest that the mechanisms of resolution and lung repair are controlled in part by regulatory pathways that are important in lung morphogenesis and development⁽⁷⁾. One of them is cell–cell interactions, which play the most important role during differentiation and tissue architecture regulation. The main members of cell–cell adhesion are cadherins, which form cell–cell adherens junctions associated with actin microfilaments via the cytoplasmic plaque proteins⁽⁸⁾. Cadherins provide mechanical cell–cell adhesion and regulate cell shape, segregation, migration, proliferation and cellular differentiation⁽⁸⁾. The interactions between cadherins and filaments of the cytoskeleton are dynamic⁽⁹⁾. Another mechanism of resolution are cytokeratins (CK), intermediate filaments (IF) of the cytoskeleton, which are

Abbreviations: CK, cytokeratins; CO, control; IF, intermediate filaments; IHCSA, immunohistochemical-stained area; PCNA, proliferating cell nuclear antigen; TGF- β 1, transforming growth factor- β 1; ZD, Zn deficiency.

* **Corresponding authors:** Dr M. S. Giménez, email mgimenez@unsl.edu.ar; Dr N. N. Gómez, email ngomez@unsl.edu.ar

expressed in tissue-specific patterns and reflect differentiation, functional specialisation and pathological alterations of the cell⁽¹⁰⁾. Desmin and vimentin also represent also IF proteins, which are related to tumour proliferation⁽¹¹⁾; however, there are few studies about the expression of these IF in the lung parenchyma.

In addition, while epithelial cell damage is largely due to the sustained effects of inflammatory mediators localised to the airways, the subsequent process of epithelial cell differentiation is attributed to members of the transmembrane receptor tyrosine kinase family called epidermal growth factor (ErbB) receptors⁽¹²⁾. Activation of the ErbB receptors induces activation and phosphorylation in cascade in cytoplasmic kinases, which results in the activation of nuclear transcription proteins, and cellular growth⁽¹³⁾.

Previously, numerous results have shown that ZD produces important changes in the expression of antioxidant enzymes and several pro-inflammatory parameters in the lung parenchyma. We think that is quite relevant to analyse it, as ZD could lead to the fibrotic process and pulmonary dysfunction. For this purpose, we set out to investigate whether the expression of these proteins during ZD is modified and if their expressions could reach the level of the control (CO) group during the period of supplementation.

Materials and methods

Diet and experimental design

Male Wistar rats (200 ± 10 g) were fed two diets with different Zn concentrations. During the pre-test, rats with similar intake profiles were matched and randomly assigned to the CO or the ZD groups (*n* 14). For that purpose, rats were divided into three groups and fed, respectively: (1) a ZD diet containing 5 mg Zn/kg and (2) a Zn-adequate CO diet containing 30 mg Zn/kg (as ZnCl₂). (3) A group of deficient animals was fed with the CO diet 10 d before killing (ZD refed group) in order to supply these animals with Zn ion. All the other components of the diet remained constant, and were supplemented with the recommended amounts of vitamins and minerals, according to the American Institute of Nutrition (AIN) 93-M diet⁽¹⁴⁾. Both diets had the following composition (g/kg): 466 maize starch, 140 casein (785 % protein), 155 dextrinised maize starch, 100 sucrose, 50 fibre/cellulose, 40 soyabean oil (containing liposoluble vitamins), 35 mineral mix AIN-93M-MX (Zn was not incorporated into the mineral mix of the ZD diet), 10 vitamin mix (AIN-93-VX), 1.8 L-cystine, 0.008 ascorbic acid, 2.5 choline bitartrate (41 % choline).

All dietary ingredients were monitored for Zn concentration using atomic absorption spectrophotometry. Animals were housed individually in a controlled environment with a 12 h light–12 h dark cycle and temperature maintained at 21 ± 2°C. Fresh diets were given and the leftover food discarded on a daily basis (20 g/d were enough to ensure ‘*ad libitum*’ feeding). All experiments were conducted in accordance with the National Institutes of Health Guide for the Care and Use of Laboratory Animals (National Institutes of Health Publication no. 80-23) and the National University

of San Luis Committee’s Guidelines for the Care and Use of Experimental Animals (Ordinance CD 006/02)⁽¹⁵⁾. Diet acclimatisation lasted 1 week, during which time the CO diet was provided to all rats and intake was measured. During the experiment, body weights were registered weekly.

Serum and tissue collection

At the second month of the treatment and 12 h after the last feeding, the animals were killed. Previously, they were anaesthetised intraperitoneally with sodium pentobarbital (50 mg/kg), and blood samples for the determination of Zn serum were collected in tubes previously washed and rinsed with nitric acid. The lungs were quickly removed, washed with ice-cold 0.9 % saline solution and weighed. Serum and pieces of lobes of each lung were frozen in liquid N₂, and then kept at –80°C until analysis. For immunochemistry, the tissue samples were fixed in 10 % buffered formalin during 6 h at room temperature and washed in PBS. For light microscopy, the fixed tissues were dehydrated in an ascending series of ethanol, cleared in xylene and embedded in paraffin. Then, 5 µm-thick sections were mounted in slides previously treated with 3-aminopropyltriethoxysilane (Sigma-Aldrich, St Louis, MO, USA) and stained with haematoxylin–eosin for preliminary observation.

Zinc analysis

Aliquots of the diet, serum and lung were collected without allowing any contact with the metal. Each sample was wet-ashed with 16 M-nitric acid, as described by Clegg *et al.*⁽¹⁶⁾. Zn concentrations of the pre-treated samples and serum were quantified by an atomic absorption spectrophotometer (model 5100, HGA-600 Graphite Furnace; Perkin-Elmer, Norwalk, CT, USA). A linear calibration curve was created using certified standard National Institute and Standards and Technology solutions. All specimens were diluted by double-distilled, deionised water, and analysed in duplicate. Before sample digestion, different amounts of the standard solution of each element were added. Recovery was between 98 and 99.2 % for different elements.

Western blot analysis for transforming growth factor-β1

Lungs were homogenised with 50 mM-Tris–HCl (pH 7.8) containing 0.01 % Triton X-100 and protease inhibitor cocktail, and centrifuged at 4°C. Protein concentrations of the resulting supernatants were determined according to the method of Wang & Smith⁽¹⁷⁾, using bovine serum albumin as the standard. Then, 40 µg of proteins were mixed with 10 µl of the sample buffer (125 mM-Tris–HCl, pH 6.8, 4 % SDS, 3.5 mM-dithiothreitol, 0.02 % bromophenol blue and 20 % glycerol), boiled for 2–3 min and loaded into a 10 % SDS–PAGE gel. Protein molecular mass markers were always loaded on each gel. Separated proteins were transferred to polyvinylidene fluoride membranes (Polyscreen NEF 1000; NEN Life Science Products, Cologne, Germany) using a blot transfer system (BioRad Laboratories, Hercules, CA, USA). After

being blocked with 5% bovine serum albumin–Tris-buffered saline solution (20 mM-Tris, 500 mM-NaCl, pH 7.5) overnight, at 4°C with gentle agitation, membranes were incubated with a primary rabbit anti-TGF- β 1 polyclonal antibody solution (1:1000 dilution; Santa Cruz Biotechnology, Inc., Santa Cruz, CA, USA) for 1 h at room temperature. After washing them three times with Tween-Tris-buffered saline (0.1% Tween 20, 100 mM-Tris-HCl, pH 7.5, 150 mM-NaCl), membranes were incubated with a secondary goat anti-rabbit IgG antibody linked to biotin for 1 h at room temperature (1:2000 dilution). β -Actin was chosen as the reference protein, over glyceraldehyde 3-phosphate dehydrogenase, for the better linearity of expression (data not shown). Membranes were washed again and the colour was developed using a Vectastain ABC detection system (Vector Laboratories, Youngstown, OH, USA). The intensity of the bands was scanned densitometrically with the image processing and analysis software Scion Image, and is expressed as arbitrary units.

Immunohistochemistry

Details of the antibodies used are provided in Table 1. Each antibody was assayed in at least three sections of each lung from each individual. A streptavidin–biotin immunoperoxidase method was performed as described previously^(18,19). After deparaffinisation, microwave pre-treatment (antigen retrieval) was performed. Endogen peroxidase activity was inhibited with 1% (v/v) H₂O₂, and non-specific binding was blocked with 10% (v/v) normal goat serum. All sections were incubated with primary antibodies for 18 h at 4°C and then for 30 min at room temperature with rat pre-absorbed, biotinylated secondary antibodies selected specifically for each of the two types of primary antibodies used (mono- or polyclonal). The visualisation of antigens was achieved by the streptavidin–peroxidase method (BioGenex, San Ramon, CA, USA), and 3,3-diaminobenzidine (Dako, Carpinteria, CA, USA) was used as chromogen. Finally, the slides were washed in distilled water, counterstained with Mayer's haematoxylin, dehydrated and mounted. To test the specificity of immunoreactions, adjacent control sections were subjected to the same immunohistochemical method, replacing primary antibodies by rabbit and mouse non-immune serum.

Image analysis

Image analysis was performed using an Image Pro-Plus 3.0.1 system (Media Cybernetics, Silver Spring, MA, USA). For the immunohistochemistry technique, images were digitised by a colour charge-coupled device (CCD) video camera (Sony, Montvale, NJ, USA) mounted on a conventional light microscope (Olympus BH-2; Olympus Company, Tokyo, Japan), using an objective magnification of 40 \times . The microscope was prepared for Koehler illumination. This was achieved by recording a reference image of an empty field for the correction of unequal illumination (shading correction) and by calibrating the measurement system with a reference slide to determine background threshold values. The reference slides contained a series of tissue sections stained in the absence

of a primary antibody. The positive controls were used as inter-assay controls to maximise the levels of accuracy and robustness of the method^(20–22). The methodological details of image analysis have been described earlier^(23,24). Using a colour segmentation analysis tool, the total intense positively stained nuclear area (brown reaction product) was measured and is expressed as a ratio (%) of the total area of cell nuclei (brown reaction product + blue haematoxylin). The image analysis score was calculated separately by using AutoPro macro language, an automated sequence operation created to measure the immunohistochemical-stained area (IHCSA). The IHCSA was calculated as a percentage of the total area evaluated through colour segmentation analysis, which extracts objects by locating all objects of a specific colour (brown stain). The brown stain was selected with a sensibility of 4 (maximum 5), and a mask was then applied to separate the colours permanently. The images were then transformed to a bi-level scale Tagged Image File Format (TIFF). The IHCSA (black area) was calculated from at least fifty images of each area of the lungs in each slide being studied.

Statistical analysis

Statistical analysis was performed using the ANOVA test when only three groups were compared⁽²⁵⁾. When variances were not homogeneous, we performed log transformation of the data. Differences between means were considered significant at the $P < 0.05$ level.

Results

Weight gain and zinc status of rats

Table 2 shows the body weight of rats fed with a ZD diet. After 2 months of treatment, body weight was significantly lower in the ZD group than in the CO group, while body weight was significantly higher in the ZD refeed group when compared with the CO group. Zn concentrations in serum and lung were significantly decreased in the ZD group; in the ZD refeed group, the level of Zn overtook the control values. The results of Zn levels are in concordance with those from the literature, i.e. El Hendy *et al.*⁽²⁶⁾. In our experimental model, clinical signs such as dermatitis or alopecia were not observed.

Table 1. Antibodies used in the present study

Antibodies	Clone	Supplier	Dilution
Primary antibodies			
CerbB-2	CerbB-2	Dako	1:300
Pan-cadherins	Pan-Cadherines	Zymed	1:50
Desmin	Desmin	Zymed	1:80
Vimentin	V-9	Zymed	1:250
CK (AE-1, AE1-3)	CK (AE-1, AE1-3)	Dako	1:100/1:700
PCNA	PC10	Novocastra	1:100
Secondary antibodies			
Anti-rabbit IgG	Polyclonal	Zymed	1:300
Anti-mouse IgG	Polyclonal	Chemicon	1:500

CK, cytokeratins; CK AE-1, monoclonal antibody anti-cytokeratins of high molecular weight; CK AE-3, monoclonal antibody anti-cytokeratins of low molecular weight; PCNA, proliferating cell nuclear antigen.

Table 2. Body and lung weight and zinc concentrations in the serum and lung of male rats

 (Mean values with their standard errors; n 14 per group)

	CO		ZD		ZD refed	
	Mean	SE	Mean	SE	Mean	SE
Body weight (g)	396	24	338*	33	407*	56
Zn in lung (ppm)	3.2	0.5	1.4*	0.2	2.2	0.4
Zn in serum (mg/l)	6.7	1.2	4.1*	0.5	7.2**	1.0

CO, control group; ZD, Zn-deficient group; ZD refed, Zn supplementation group; ppm, parts per million.

 Mean value was significantly different from that of the CO group: * $P < 0.05$, ** $P < 0.01$ (ANOVA).

Expression of transforming growth factor- β 1

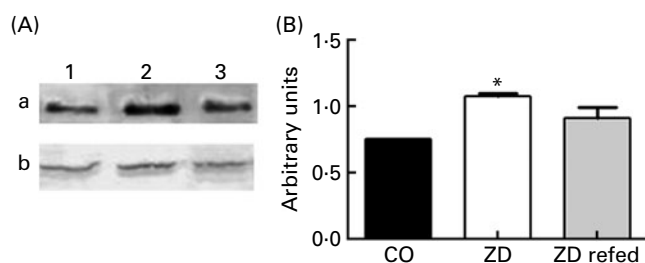
TGF- β 1 is the most important cytokine promoting the development of fibrosis in the lung. It has multiple functions in repair, wound healing, during organogenesis and development; for this reason, we measured this factor. Fig. 1 shows the increased expression of TGF- β 1 in the ZD group when compared with the CO group.

Immunohistochemistry

Factor *CerbB-2* immunostaining. Factor *CerbB-2* was observed in the cytoplasm of cells in all groups treated. In the CO group, moderate staining was observed. Immunoreactivity in the ZD and ZD refed groups was significantly higher ($P < 0.05$) compared with the CO group (Table 3). The data also revealed the presence of weak cytoplasmic staining in the cells and alveolar spaces in the pulmonary parenchyma; this staining was considered as part of the background, and it was not included in the analysis (Fig. 2(A)–(C)).

Pan-cadherin immunostaining. The results of the quantitative image analysis of pan-cadherin immunostaining (IHCSA) are shown in Table 3. Immunostaining did not show significant differences between all treated groups (Fig. 2(D)–(F)).

Cytokeratin immunostaining. CK showed a low expression in ZD lungs, while in the ZD refed group, the expression of CK was significantly increased ($P < 0.05$) compared with the CO group (Table 3; Fig. 2(G)–(I)).


Fig. 1. Immunoblot analysis of tumour growth factor β (TGF- β 1) expression in the lung. (A) Representative experiment of Western blot is shown. (a) TGF- β 1 expression was detected with an anti-TGF- β 1 antibody. (b) β -Actin was used as a reference protein. (B) Quantification of the protein band corresponding to TGF- β 1 was performed by densitometry. Results show the intensity of the TGF- β 1 band in relation to the intensity of a reference protein band (n 14 per dietary group). *Mean value was significantly different from that of the control group ($P < 0.05$).

Desmin immunostaining. Desmin was observed in the cytoplasm of all cells in each treated group. Immunoreactivity did not show significant differences between all groups (Table 3; Fig. 3(D)–(F)).

Vimentin immunostaining. The results of the quantitative image analysis of vimentin immunostaining are shown in Table 3. Vimentin was detected in the cytoplasm of cells in all groups. In the ZD refed group, immunostaining was significantly higher ($P < 0.05$) compared with the CO group (Fig. 3(A)–(C)).

Proliferating cell nuclear antigen immunostaining. Proliferating cell nuclear antigen (PCNA) was observed in the cytoplasm of cells in all groups treated. In the CO group, moderate staining was observed. Immunoreactivity in the ZD and ZD refed groups was significantly higher ($P < 0.05$) compared with the CO group (Table 3; Fig. 3(G)–(I)).

Discussion

Zn is known to exert antioxidant effects *in vitro* and *in vivo*, although Zn itself is redox inert^(5,27). On the other hand, Zn deficiency as well as Zn overload may induce oxidative stress and may be cytotoxic^(5,27). While Zn supplementation protects from oxidative stress in many different cell types, as well as in animal models^(5,28,29), Zn deprivation has been found to increase intracellular oxidative stress and to induce apoptotic cell death^(5,30). We have previously showed that ZD induce an important oxidative and nitrosative stress in the lung parenchyma^(5,6) and demonstrated that NO-related species are accumulated in the lung during the course of Zn deficiency⁽⁵⁾.

Taking into account studies previously undertaken by different groups as a result of a Zn deficiency, we decided to investigate what was happening in the cytoskeleton under these conditions. In addition, a group of animals with the CO diet was refed for 10 d in order to determine whether there was a recovery of some of the studied parameters.

We used an experimental model that has the advantage of being used for a long time to obtain more relevant physiological results^(31,32). In our experimental design, Zn deprivation for 8 weeks induces a decrease in body weight in the ZD group. Zn is known to play a role in protein metabolism^(33–35) and has been identified that Zn deficiency produces deficient

Table 3. Percentage of the immunostaining area in the lung with different antibodies used in immunohistochemistry

 (Mean values with their standard errors; n 14 per group)

	CO		ZD		ZD refed	
	Mean	SE	Mean	SE	Mean	SE
Factor <i>CerbB-2</i>	17.53	6.40	31.90**	11.57	31.68**	9.69
Pan-cadherins	23.29	7.07	29.10	8.82	34.87	8.94
Cytokeratins	11.70	1.68	6.07	3.66	21.61**	6.88
Desmin	39.20	5.27	42.28	5.60	45.12	10.72
Vimentin	6.58	1.90	9.05	4.99	15.54**	8.29
PCNA	4.82	1.11	9.63**	2.74	10.21**	3.30

 CO, control group; ZD, Zn-deficient group; ZD refed, Zn supplementation group; *CerbB-2*, epidermal growth factor receptor; PCNA, proliferating cell nuclear antigen. **Mean value was significantly different from that of the CO group ($P < 0.01$; ANOVA).

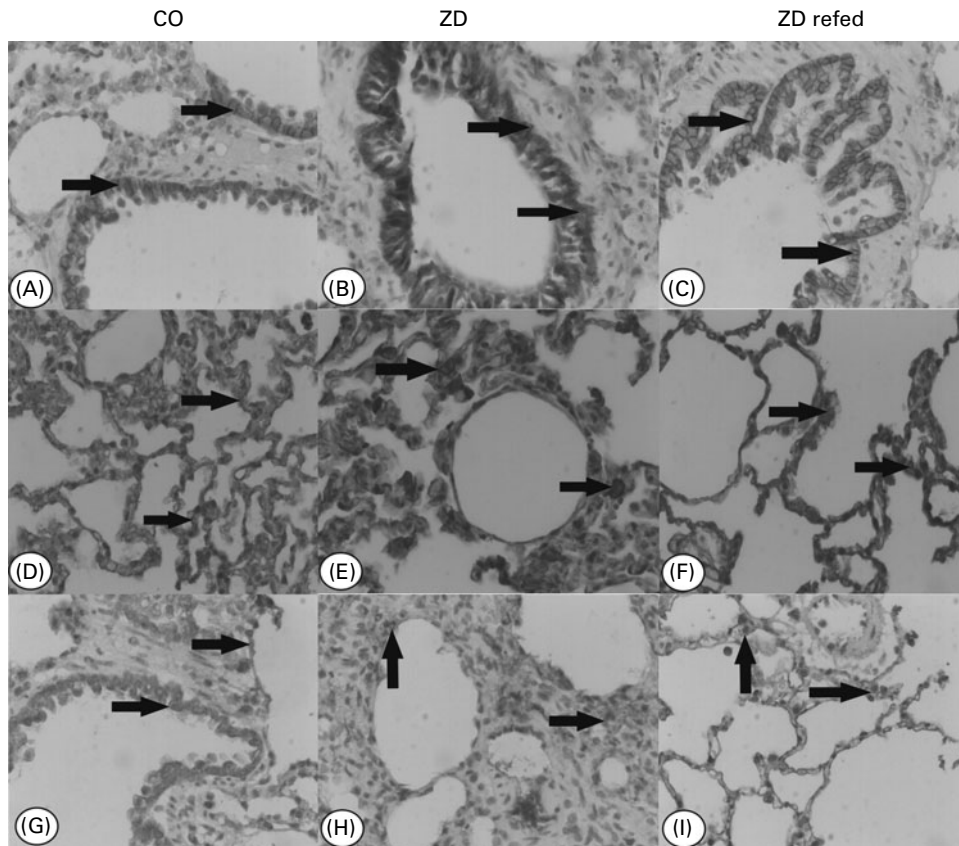


Fig. 2. Immunohistochemical findings of CerbB-2, pan-cadherins and cykeratins (CK) in the lung parenchyma of the control (CO), zinc deficiency (ZD) and ZD refeed groups. (A)–(C) CerbB-2 expression in the cytoplasmic regions (arrows). (D)–(F) Pan-cadherin expression is present in the alveolar cells and capillary wall (arrows). (G)–(I) Positive immunostaining for CK (arrows), 40 ×.

protein digestion and absorption. Yu *et al.*⁽³⁶⁾ also proposed that Zn deficiency affects the growth and development of bones, which could be another factor in the final body weight of the animals. Zn refeeding restores body weight in the ZD refeed group (Table 1).

A decrease in serum Zn increased the risk for developing metabolic and clinical signs of Zn deficiency⁽³⁷⁾ and confirmed previous data^(5,33). During the supplementation period, serum Zn concentration increased in relation to ZD. Some authors have shown the fact that, when Zn is added back to the diet, growth is promptly resumed, and it initially proceeds even faster than in the controls⁽³⁸⁾; the time of refeeding used in the present study was enough to overtake the normal level of Zn.

The alveolar epithelium serves as a major source of TGF- β 1 and many other cytokines including TNF- α , during lung injury and fibrosis⁽³⁸⁾. The alveolar epithelium also regulates an intrinsic capacity to respond to TGF- β 1 stimulation through the differential expression of TGF- β 1 receptor subtypes⁽³⁹⁾. Taken together, these data suggest that the alveolar epithelium plays a major role in the pathogenesis of lung fibrosis, with the capacity to produce and respond to TGF- β 1, and modify cell morphology and gene expression in response to injury, all independent of the degree of inflammation. On the other hand, Moustakas & Heldin⁽⁴⁰⁾ demonstrated that TGF- β

members have a strong and complex impact on the organisation of the cytoskeleton architecture. This primarily involves the actin cytoskeleton and, secondarily, certain systems of IF⁽⁴¹⁾. TGF- β signalling seems to aim at least two different physiological outcomes that are interlinked: first, it changes the overall cellular architecture that has an impact on differentiation and, second, facilitates cell motility, prerequisites of which are altered architectural arrangement and the remodelling of the extracellular matrix. Considering these facts, the increased expression of TGF- β 1 during ZD may lead to remodelling process activation in the lung parenchyma. However, the relationship between the production of growth factors by the airway epithelium and the subsequent remodelling remains poorly understood.

We have previously demonstrated an increase in the gene transcription of many inflammatory cytokines such as TNF- α during Zn deficiency. In agreement with this, an important infiltration of inflammatory cells, principally, neutrophils (data not shown) was observed in our experimental model⁽⁶⁾. Besides, some authors have shown the relationship between TNF- α and other fibrogenic molecules with a fibrotic sequel, in particular TGF- β 1. TGF- β 1 is up-regulated in pathologies in which TNF- α is associated with fibrosis^(40,42). Recent evidence indicates that some matrix metalloproteinases

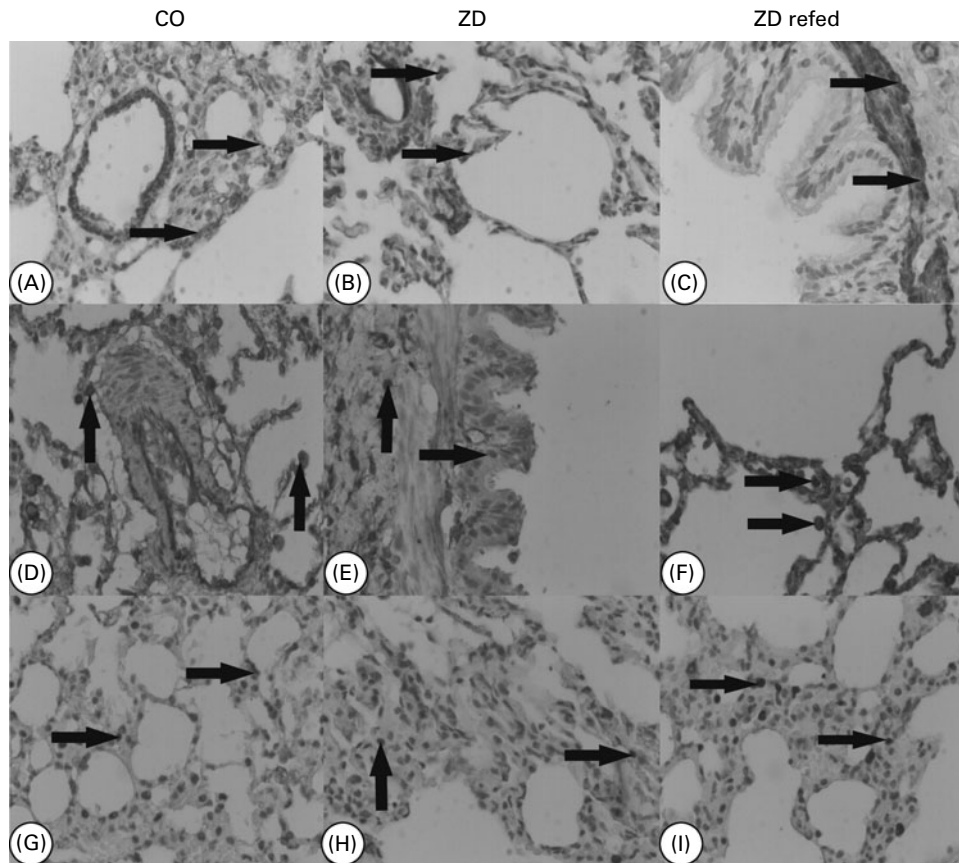


Fig. 3. Immunohistochemical findings of vimentin, desmin and proliferating cell nuclear antigen (PCNA) in the lung parenchyma of the control (CO), zinc deficiency (ZD) and ZD refed groups. (A)–(C) Positive cytoplasmic immunostaining of vimentin (arrows). (D)–(F) Desmin immunostaining in the cytoplasmic cell regions (arrows). (G)–(I) Nuclear expression of PCNA protein (arrows), 40 × .

are implicated in the cancer process, with infiltration of inflammatory cells and metastasis⁽⁴³⁾.

In our model, the immunostaining of the CerbB-2 factor (Table 3), an epithelial protein that induces the proliferation and differentiation of cells⁽⁴⁴⁾, was increased in the ZD and ZD refed groups. According to the evidence, we can suggest that the increased expression of CerbB-2 during Zn deficiency and ZD refeeding is associated with cell proliferation processes, perhaps in order to promote the remodelling of the respiratory epithelium.

Chilosi *et al.*⁽⁴⁵⁾ and Willis *et al.*⁽⁴⁶⁾ indicated that there are several pathways of remodelling during lung morphogenesis, including the action of these proteins; however, during a state of injury, the repair process may be altered, leading to fibrosis⁽⁴⁷⁾. Within the pan-cadherins, β -catenin is one of the most important proteins because of its role in cell migration and adhesion by direct interaction with the cytoskeleton⁽⁴⁶⁾. Several experiments have shown that this protein is expressed in epithelial cells type II when it induces a state of hypoxia in rats⁽⁴⁸⁾. The present findings show a slight increase in pan-cadherins in the ZD refed group; this situation could be attributed to increased cell proliferation by promoting cell–cell adhesion. However, the expression of these proteins during Zn deficiency was not altered, which would suggest

that this deficiency does not affect the integrity of cell–cell junctions.

Furthermore, the expression of CK in ZD remained unchanged; however, we showed evidence for lung epithelial damage during Zn deficiency. In the ZD refed group, the expression of these proteins increased when compared with the CO group (Table 3); this situation suggested a possible reactivation of mesothelial cells, presumably in order to repair the damaged epithelium.

On the other hand, desmin (a member of the cytoskeleton) is present in smooth muscle cells, skeletal cardiac cells, as well as in myoepithelial cells^(49,50). Most of the background found in the literature relates the presence of vimentin and desmin in the development of the carcinogenic process, where these proteins would be used as markers of proliferation. In our experimental model, desmin expression did not change in all treated groups (Table 3), which could suggest that cells with myoepithelial origin would not be affected during Zn deficiency.

The present study also showed that the immunostaining of PCNA-positive cells in the ZD and ZD refed groups was higher compared with the CO group (Table 3). Interestingly, it has been found that the PCNA expression level correspondingly increased in regions of the high expression of inducible NO synthase⁽⁵¹⁾. In fact, our previous study has shown an increase

in inducible NO synthase and endothelial NO synthase expression in ZD lung during Zn deficiency. Inducible NO synthase immunostaining was detected in alveolar type II cells and polymorphonuclear neutrophils (data not shown). Besides, recently, evidence has shown that PCNA and E-cadherin (pan-cadherin family) play an important role in the invasion and metastasis of cancer.⁽⁵²⁾

There is evidence that helps us to understand even more the effect of Zn deficiency on the epithelium. Nickolson & Veldstra⁽⁵³⁾ demonstrated the effect of Zn deficiency and oxidative stress on the microtubules; they demonstrated the deregulation of the normal functions of the cytoskeleton⁽⁵⁴⁾. It has also been observed that mesothelial cells are stimulated with high concentrations of glucose or pro-inflammatory cytokine that induces the expression of TGF- β and decreases the expression of E-cadherin⁽⁵³⁾, which plays a key role in the control of the epithelial–mesenchymal transition^(55,56). Additionally, MacKenzie *et al.*⁽⁵⁷⁾ showed that in cultured neuronal cells with Zn deficiency, there was an alteration of the processes of neuronal differentiation and proliferation, which was reflected in the cytoskeleton, and a decrease in translocation NF- κ B⁽⁵⁸⁾. Moreover, the excessive production of reactive oxygen species is associated with the activation of pro-fibrogenic genes in cells producing collagen⁽⁴⁾. The production of reactive oxygen species has previously been shown in our experimental model^(5,6). In addition, damage to respiratory epithelial cells is related to interstitial oedema, PMN invasion and decreased lung capacity^(57,59); the inflammatory status factor causes the activation of TGF- β , which in turn induces the activation of fibroblasts.

Bringardner *et al.*⁽⁶⁰⁾ demonstrated that the inflammatory process affects the structure of the extracellular matrix, the secretion of receptors for growth factors and cellular plasticity; therefore, an increase in the degree of cellular plasticity is associated with the presence of fibrosis⁽⁶¹⁾. In fact, in our experimental model, we have shown that Zn deficiency would generate a severe inflammatory condition, which would lead to a deterioration of the respiratory epithelium, a situation which is characterised by the accumulation of inflammatory cells in the pulmonary stroma⁽⁵⁾, and an increased expression of pro-inflammatory parameters⁽⁶⁾. Taken together, this evidence suggests that Zn deficiency provokes a critical damage to the alveolar epithelium, which, at least in part, could be recovered by connective tissue during the refeeding time.

In conclusion, the changes observed are probably due to structural and functional alterations that occur during Zn deficiency and may be associated with important modifications in the expression of cytoskeleton proteins and cellular adhesion molecules. Besides, the presence of fibrosis significantly increases the risk of the development of tumour foci in the lung. Finally, when this situation occurs together with other pathologies, it could lead to a worse prognosis.

Acknowledgements

This study was supported by a grant from the National Scientific and Technical Research Council (CONICET)-22Q614 and the Secretary of Science and Technology (SECyT)-Project

8104-National University of San Luis, Argentina. All authors declare that they have no commercial/financial conflict of interest. The authors would like to thank Dr A. Acosta for valuable atomic absorption spectrophotometer contribution; Dr J. Chediak for his excellent assistance in the Western blotting technique and Dr R. Dominguez for her technical assistance. The specific collaboration of each contributing author was as follows: V. S. B. and N. N. G. contributed to the experimental design and manuscript writing. V. S. B. and M. V. P. C. performed all the molecular biology experiments. S. R. V. was involved in the histological preparation of tissues. V. S. B., N. R. S. and H. H. O. collaborated on the immunohistochemistry technique. M. S. G. was the Project Director.

References

1. Cortese MM, Suschek CV, Wetzel W, *et al.* (2008) Zinc protects endothelial cells from hydrogen peroxide via Nrf2-dependent stimulation of glutathione biosynthesis. *Free Radical Biol Med* **44**, 2002–2012.
2. Truong-Tran AQ, Ruffin RE & Zaleski PD (2000) Visualization of labile zinc and its role in apoptosis of primary airways epithelial cells and cell lines. *Am J Physiol Lung Cell Mol Physiol* **279**, L1172–L1183.
3. Beattie JH & Kwun IS (2004) Is zinc deficiency a risk factor for atherosclerosis? *Br J Nutr* **91**, 177–181.
4. Kisseleva T & Brenner DA (2008) Mechanisms of fibrogenesis. *Exp Biol Med (Maywood)* **233**, 109–122.
5. Gomez NN, Davicino RC, Biaggio VS, *et al.* (2006) Overexpression of inducible nitric oxide synthase and cyclooxygenase-2 in rat zinc-deficient lung: Involvement of a NF- κ B dependent pathway. *Nitric Oxide* **14**, 30–38.
6. Biaggio VS, Pérez Chaca MV, Valdéz SR, *et al.* (2010) Alteration in the expression of inflammatory parameters as a result of oxidative stress produced by moderate zinc deficiency in rat lung. *Exp Lung Res* **36**, 31–44.
7. Willis BC, Liebler JM, Luby-Phelps K, *et al.* (2005) Induction of epithelial-mesenchymal transition in alveolar epithelial cells by transforming growth factor-beta1: potential role in idiopathic pulmonary fibrosis. *Am J Pathol* **166**, 1321–1332.
8. Gloushankova NA (2008) Changes in regulation of cell-cell adhesion during tumor transformation. *Biochemistry (Mosc)* **73**, 742–750.
9. Drees F, Pokutta S, Yamada S, *et al.* (2005) Alpha-catenin is a molecular switch that binds E-cadherin-beta-catenin and regulates actin-filament assembly. *Cell* **123**, 903–915.
10. Iyonaga K, Miyajima M, Suga M, *et al.* (1997) Alterations in cytokeratin expression by the alveolar lining epithelial cells in lung tissues from patients with idiopathic pulmonary fibrosis. *J Pathol* **182**, 217–224.
11. Hockfield S & McKay RD (1985) Identification of major cell classes in the developing mammalian nervous system. *J Neurosci* **5**, 3310–3328.
12. Damera G, Xia B, Ancha HR, *et al.* (2006) IL-9 modulated MUC4 gene and glycoprotein expression in airway epithelial cells. *Biosci Rep* **26**, 55–67.
13. Hamilton A & Piccart M (2000) The contribution of molecular markers to the prediction of response in the treatment of breast cancer: A review of the literature on HER-2, p53 and BCL-2. *Ann Oncol* **11**, 647–663.
14. Reeves PG, Nielsen FH & Fahey GC Jr (1993) AIN-93 purified diets 785 for laboratory rodents: final report of the American Institute of Nutrition *ad hoc* writing committee on the reformulation of the AIN-76A rodent diet. *J Nutr* **123**, 1939–1951.



15. US Public Health Service (1985) *Guide to the Care and Use of Laboratory Animals*, pp. 85–123. Bethesda, MD: National Institutes of Health.
16. Clegg MS, Keen CL & Lonnerdal B (1981) Influence of ashing techniques on the analysis of trace elements in animal tissue. I Wet ashing. *Biol Trace Elem Res* **3**, 107–115.
17. Wang C & Smith RL (1975) Lowry determination of protein in the presence of Triton X-100. *Anal Biochem* **63**, 414–417.
18. Salvetti NR, Gimeno EJ, Lorente JA, *et al.* (2004) Expression of cytoskeletal proteins in the follicular wall of induced ovarian cysts. *Cells Tissues Organs* **178**, 117–125.
19. Ortega HH, Lorente JA, Mira GA, *et al.* (2004) Constant light exposure cause dissociation in gonadotropins secretion and inhibits partially neuroendocrine differentiation of Leydig cells in adult rats. *Reprod Domest Anim* **39**, 417–423.
20. Ranefall P, Wester K & Bengtsson E (1998) Automatic quantification of immunohistochemically stained cell nuclei using unsupervised image analysis. *Anal Cell Pathol* **16**, 29–43.
21. Ortega HH, Salvetti NR, Muller LA, *et al.* (2007) Characterization of cytoskeletal proteins in follicular structures of cows with cystic ovarian disease. *J Comp Pathol* **136**, 222–230.
22. Salvetti NR, Muller LA, Acosta JC, *et al.* (2007) Estrogen receptors a and b and progesterone receptors in ovarian follicles of cows with cystic ovarian disease. *Vet Pathol* **44**, 373–378.
23. Wang H, Masironi B, Eriksson H, *et al.* (1999) A comparative study of estrogen receptors a and b in the rat uterus. *Biol Reprod* **61**, 955–964.
24. Wang H, Eriksson H & Sahlin L (2000) Estrogen receptors a and b in the female reproductive tract of the rat during the estrous cycle. *Biol Reprod* **63**, 1331–1340.
25. Denenberg VH (1984) Some statistical and experimental considerations in the use of the analysis-of-variance procedure. *Am J Physiol* **246**, R403–R408.
26. El Hendy HA, Yousef MI & Abo El-Naga NI (2001) Effect of dietary zinc deficiency on hematological and biochemical parameters and concentrations of zinc, copper, and iron in growing rats. *Toxicology* **167**, 163–170.
27. Krezel A, Hao Q & Maret W (2007) The zinc/thiolate redox biochemistry of metallothionein and the control of zinc ion fluctuations in cell signaling. *Arch Biochem Biophys* **463**, 188–200.
28. Sahin K, Smith MO, Onderci M, *et al.* (2005) Supplementation of zinc from organic or inorganic source improves performance and antioxidant status of heat-distressed quail. *Poult Sci* **84**, 882–887.
29. Bediz CS, Baltaci AK, Mogulkoc R, *et al.* (2006) Zinc supplementation ameliorates electromagnetic field-induced lipid peroxidation in the rat brain. *Toboku J Exp Med* **208**, 133–140.
30. Ho E, Courtemanche C & Ames BN (2003) Zinc deficiency induces oxidative DNA damage and increases p53 expression in human lung fibroblasts. *J Nutr* **133**, 2543–2548.
31. Gomez NN, Fernandez MR, Zirulnik F, *et al.* (2003) Chronic zinc deficiency induces an antioxidant adaptive response in rat lung. *Exp Lung Res* **29**, 485–502.
32. Cunnane SC & Yang J (1995) Zn deficiency impairs whole-body accumulation of polyunsaturates and increases the utilization of [1–14C] linoleate for *de novo* lipid synthesis in pregnant rats. *Can J Physiol Pharmacol* **73**, 1246–1252.
33. Gómez NN, Ojeda MS & Gimenez MS (2002) Lung lipid composition in zinc-deficient rats. *Lipids* **37**, 291–296.
34. Yousef MI, El Hendy HA, El Demerdash FM, *et al.* (2002) Dietary zinc deficiency induced changes in the activity of enzymes and the levels of free radicals, lipids and protein electrophoretic behavior in growing rats. *Toxicology* **175**, 223–234.
35. Ying AJ, Shu XL, Gu WZ, *et al.* (2011) Effect of zinc deficiency on intestinal mucosal morphology and digestive enzyme activity in growing rat. *Zhonghua Er Ke Za Zhi* **49**, 249–254.
36. Yu XD, Yan CH, Yu XG, *et al.* (2005) Effect of zinc deficiency on femoral pathological and morphological changes in growth-term rats. *Wei Sheng Yan Jiu* **34**, 178–180.
37. King JC (1990) Assessment of zinc status. *J Nutr* **120**, Suppl. 11, 474–1479.
38. Dorup I & Clausen T (1991) Effects of magnesium and zinc deficiencies on growth and protein synthesis in skeletal muscle and the heart. *Br J Nutr* **66**, 493–504.
39. Xu YD, Hua J, Mui A, *et al.* (2003) Release of biologically active TGF-beta1 by alveolar epithelial cells results in pulmonary fibrosis. *Am J Physiol* **285**, L527–L539.
40. Moustakas A & Heldin CH (2008) Dynamic control of TGF- β signaling and its links to the cytoskeleton. *FEBS Lett* **582**, 2051–2065.
41. Khalil N, Parekh TV, O'Connor RN, *et al.* (2002) Differential expression of transforming growth factor β type I and II receptors by pulmonary cells in bleomycin-induced lung injury. *Exp Lung Res* **28**, 233–250.
42. Phan SH & Kunkel SL (1992) Lung cytokine production in bleomycin-induced pulmonary fibrosis. *Exp Lung Res* **18**, 29–43.
43. Kapanci Y, Desmouliere A, Pache JC, *et al.* (1995) Cytoskeletal protein modulation in pulmonary alveolar myofibroblasts during idiopathic pulmonary fibrosis: possible role of TGF- β and TNF- α . *Am J Respir Crit Care Med* **152**, 2163–2169.
44. Egeblad M & Werb Z (2002) New functions for the matrix metalloproteinases in cancer progression. *Nat Rev Cancer* **2**, 161–174.
45. Chilosi M, Poletti V, Murer B, *et al.* (2002) Abnormal re-epithelialization and lung remodeling in idiopathic pulmonary fibrosis: the role of deltaN-p63. *Lab Invest* **82**, 1335–1345.
46. Willis BC, duBois RM & Borok Z (2006) Epithelial origin of myofibroblasts during fibrosis in the lung. *Proc Am Thorac Soc* **3**, 377–382.
47. Hynes NE & Lane HA (2005) ERBBreceptors and cancer: the complexity oft argeted inhibitors. *Nat Rev Cancer* **5**, 341–354.
48. Douglas IS, Diaz del Valle F, Winn RA, *et al.* (2006) B-catenin in the proliferative response to acute lung injury. *Am J Respir Cell Mol Biol* **34**, 274–285.
49. Reddy R, Buckley S, Doerken M, *et al.* (2004) Isolation of a putative progenitor subpopulation of alveolar epithelial type 2 cells. *Am J Physiol Lung Cell Mol Physiol* **286**, L658–L667.
50. Osborn L, Hession C, Tizard R, *et al.* (1989) Direct expression cloning of vascular cell adhesion molecule 1, a cytokine-induced endothelial protein that binds to lymphocytes. *Cell* **59**, 1203–1211.
51. Yang YG & Makita T (1996) Immunocytochemical localization of Desmin and Vimentin in human fetal skeletal-muscle cells. *Anat Rec* **246**, 64–70.
52. Sang JR, Chen YC, Shao GB, *et al.* (2010) Effect of nitric oxide on the proliferation of AGS gastric cancer cells. *Chin J Cancer* **29**, 158–162.
53. Nickolson VJ & Veldstra H (1972) The influence of various cations on the binding of colchicine by rat brain homogenates. Stabilization of intact neurotubules by zinc and cadmium ions. *FEBS Lett* **23**, 309–313.



54. Weng MX, Wu CH & Yang XP (2008) Expression and significance of E-cadherin, CD44v6, and proliferating cell nuclear antigen in non-small cell lung cancer. *Ai Zheng* **27**, 191–195.
55. Yang WS, Kim BS, Lee SK, *et al.* (1999) Interleukin 1b stimulates the production of extracellular matrix in cultured human peritoneal mesothelial cells. *Perit Dial Int* **19**, 211–220.
56. Perl AK, Wilgenbus P, Dahl U, *et al.* (1998) A causal role for E-cadherin in the transition from adenoma to carcinoma. *Nature* **392**, 190–193.
57. Mackenzie GG, Keen CL & Oteiza PI (2006) Microtubules are required for NF- κ B nuclear translocation in neuroblastoma IMR-32 cells: modulation by zinc. *J Neurochem* **2**, 402–415.
58. Takeichi M (1995) Morphogenic roles of classic cadherins. *Curr Opin Cell Biol* **7**, 619–627.
59. Kuwano K, Hagimoto N & Nakanishi Y (2004) The role of apoptosis in pulmonary fibrosis. *Histol Histopathol* **9**, 867–881.
60. Bringardner BD, Baran CP, Eubank TD, *et al.* (2008) The role of inflammation in the pathogenesis of idiopathic pulmonary fibrosis. *Antioxid Redox Signal* **10**, 287–302.
61. Strieter RM, Gomperts BN & Keane MP (2007) The role of CXC chemokines in pulmonary fibrosis. *J Clin Invest* **117**, 549–556.